ACS APPLIED BIO MATERIALS
Cite This: ACS Appl. Bio Mater. 2019, 2, 4044−4051
Article
www.acsabm.org

Behavior of *E. coli* with Variable Surface Morphology Changes on Charged Semiconductor Interfaces

Divya Iyer,[‡] Alexey V. Gulyuk,[†] Pramod Reddy,[§] Ronny Kirste,[§] Ramon Collazo,[†] Dennis R. LaJeunesse,[*,‡] and Albena Ivanisevic[*,†]

[†]Department of Materials Science and Engineering, North Carolina State University, Raleigh, North Carolina 27695, United States
[‡]Department of Nanoscience, Joint School of Nanoscience and Nanoengineering, University of North Carolina-Greensboro, Greensboro, North Carolina 27401, United States
[§]Adroit Materials, 2054 Kildaire Farm Road, Suite 205, Cary, North Carolina 27518, United States

Supporting Information

ABSTRACT: Bacterial behavior is often controlled by structural and composition elements of their cell wall. Using genetic mutant strains that change specific aspects of their surface structure, we modified bacterial behavior in response to semiconductor surfaces. We monitored the adhesion, membrane potential, and catalase activity of the Gram-negative bacterium *Escherichia coli* (*E. coli*) that were mutant for genes encoding components of their surface architecture, specifically flagella, fimbriae, curli, and components of the lipopolysaccharide membrane, while on gallium nitride (GaN) surfaces with different surface potentials. The bacteria and the semiconductor surface properties were recorded prior to the biofilm studies. The data from the materials and bioassays characterization supports the notion that alteration of the surface structure of the *E. coli* bacterium resulted in changes to bacterium behavior on the GaN medium. Loss of specific surface structure on the *E. coli* bacterium reduced its sensitivity to the semiconductor interfaces, while other mutations increase bacterial adhesion when compared to the wild-type control *E. coli* bacteria. These results demonstrate that bacterial behavior and responses to GaN semiconductor materials can be controlled genetically and can be utilized to tune the fate of living bacteria on GaN surfaces.

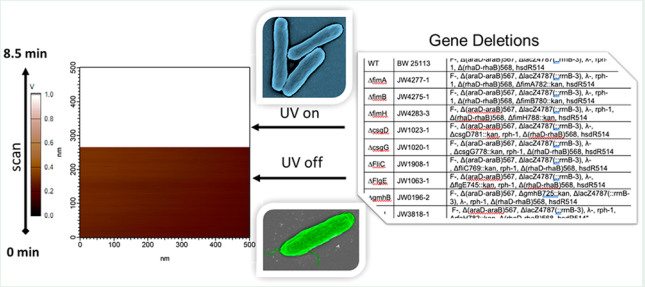

KEYWORDS: *gallium nitride, E. coli, UV light, Kelvin probe force microscopy, membrane potential, catalase, cell adhesion*

1. INTRODUCTION

The structure of bacteria is dynamic and capable of responding to various external stimuli that can be of a chemical or mechanical nature.[1,2] Certain bacteria like the Gram-negative bacterium, *Escherichia coli* (*E. coli*), efficiently respond to external stimuli by alteration of their surface composition and morphology.[3] Structures such as flagella, pili, curli, and lipopolysaccharide (LPS) complex participate in signaling-related functions.[4] Mechanical signals from the extracellular environment are transduced through the bacterial cell wall via the LPS, a complex matrix composed ofoligosaccharide O-antigen, inner core, and lipid layer, lipid-A.[5,6] Flagella participate in motility, but also "feel out" crevices for adhesion.[7,8] Bacteria surface structures also are essential during biofilm formation with their roles documented in the literature as the following: flagella, structures associated for motility and surface sensing;[8,9] pili/fimbriae, adhesive structures;[10,11] curli, structures with roles in adhesion, aggregation, and colony formation;[12,13] and LPS (permeability barrier and virulence).[6] Differences and changes in the bacterial surface morphology via appendage changes alter subsequent interactions with interfaces. Understanding the bacterial interactions with interfaces is particularly important for several practical problems associated with health and the environment. While a number of studies have focused on interfaces made of polymeric and metal surfaces associated with biomedical applications,[14] a relatively smaller number of studies have examined interactions of *E. coli* with semiconductor materials.

Understanding the interactions of microorganisms with semiconductors will lead to new paradigms in the field of bioelectronics.[15,16] In particular, there are a number of unique semiconductor properties that can be utilized to influence the behavior of cells on these interfaces.[17] We have recently reported on the favorable biocompatibility properties of III-nitrides and the ability to tune adhesion via topography and surface chemistry.[18] However, these semiconductors also have persistent photoconductivity associated with the accumulation of surface charge and a change in surface potential that persist with long lifetime even after the source used for photo-activation, such as UV light, is removed. We have shown that

Received: June 28, 2019
Accepted: August 13, 2019
Published: August 13, 2019

DOI: 10.1021/acsabm.9b00573
ACS Appl. Bio Mater. 2019, 2, 4044−4051

photoactivated gallium nitride (GaN) materials alter cell adhesion, plasma membrane potential, cell physiology, biofilm formation, and mitochondrial activity.[19,20] We have collected evidence that some of the observed cell behavior can be explained by the generation of locally high levels of reactive oxygen species (ROS) on the surface.[21] However, there is a need to understand what structural aspects of the bacterial cell also contribute to the biological response upon interaction with a semiconductor interface.

In this study, we show that changes to the bacterial surface morphology alter the behavior of *E. coli* on GaN surfaces that have been previously exposed to UV light. We examine the behavior of *E. coli* that contained deletions for genes that are associated with specific surface structures (Table 1).

Table 1. *E. coli* Strains and Genotypes Utilized in the Study

name	keio library strain #	genotype
WT	BW 25113	*F-, Δ(araD-araB)567, ΔlacZ4787(::rrnB-3), λ-, rph-1, Δ(rhaD-rhaB)568, hsdR514*
Δ*fimA*	JW4277-1	*F-, Δ(araD-araB)567, ΔlacZ4787(::rrnB-3), λ-, rph-1, Δ(rhaD-rhaB)568, ΔfimA782::kan, hsdR514*
Δ*fimB*	JW4275-1	*F-, Δ(araD-araB)567, ΔlacZ4787(::rrnB-3), λ-, rph-1, Δ(rhaD-rhaB)568, ΔfimB780::kan, hsdR514*
Δ*fimH*	JW4283-3	*F-, Δ(araD-araB)567, ΔlacZ4787(::rrnB-3), λ-, rph-1, Δ(rhaD-rhaB)568, ΔfimH788::kan, hsdR514*
Δ*csgD*	JW1023-1	*F-, Δ(araD-araB)567, ΔlacZ4787(::rrnB-3), λ-, ΔcsgD781::kan, rph-1, Δ(rhaD-rhaB)568, hsdR514*
Δ*csgG*	JW1020-1	*F-, Δ(araD-araB)567, ΔlacZ4787(::rrnB-3), λ-, ΔcsgG778::kan, rph-1, Δ(rhaD-rhaB)568, hsdR514*
Δ*fliC*	JW1908-1	*F-, Δ(araD-araB)567, ΔlacZ4787(::rrnB-3), λ-, ΔfliC769::kan, rph-1, Δ(rhaD-rhaB)568, hsdR514*
Δ*flgE*	JW1063-1	*F-, Δ(araD-araB)567, ΔlacZ4787(::rrnB-3), λ-, ΔflgE745::kan, rph-1, Δ(rhaD-rhaB)568, hsdR514*
Δ*gmhB*	JW0196-2	*F-, Δ(araD-araB)567, ΔgmhB725::kan, ΔlacZ4787(::rrnB-3), λ-, rph-1, Δ(rhaD-rhaB)568, hsdR514*
Δ*rfaH*	JW3818-1	*F-, Δ(araD-araB)567, ΔlacZ4787(::rrnB-3), λ-, rph-1, ΔrfaH783::kan, Δ(rhaD-rhaB)568, hsdR514″*

Specifically, we selected genes that encode components of the fimbriae, which are thin, rigid, polar filaments that protrude from the surface of the bacteria. Fimbriae are composed of the long-chain protein, pilin, and are known to be responsible for forming the initial stable cell-surface attachments in a concentration dependent manner.[22] Alteration to the structure of the fimbriae changes the adhesive potential of bacteria.[23] We also examined bacteria deficient in genes that encode curli-thin, intrinsic proteinaceous components of the outer membrane that play a role in cell aggregation.[24] Curli production is highly regulated and responsible for the transition from a predominantly flagellar-based motile behavior to curli-enhanced adhesive processes during the initial formation of a biofilm.[5,13,24] Unlike fimbriae, there is no relationship between the curli concentration and adhesion. Finally, we examined the role that flagella, the long tubular helix composed of the protein flagellin, plays in motility and mechano-sensation.[25,26] In this report, we characterize separately the semiconductor and bacterial surfaces, and subsequently relate their properties to changes in *E. coli* behavior on UV-treated (UV+) and nontreated (UV-) GaN with respect to cell adhesion, membrane potential, and catalase activity.

2. RESULTS AND DISCUSSION

2.1. *E. coli* Interfaces. Prior to the evaluation of the behavior of the mutated *E. coli* on the semiconductor surfaces, we gathered data to understand the interfacial properties of 10 strains. We studied the deletion mutations of the three major fimbriae genes: *fimA*, *fimB*, and *fimH*. The *fimA* gene encodes the major repeating protein subunit of the fimbriae and deletions of the *fimA* gene lead to the loss of fimbriae formation.[10] The *fimB* gene encodes a transcriptional regulator of *fimA*, and in the absence of FimB function, one observes no FimA production.[27] The *fimH* encodes a minor component of the fimbriae proper that is required for governing the length and adhesive properties of fimbriae and the loss of FimH results in altered adhesion.[28] We examined the deletions of curli formation genes: *csgG* and *csgD*. The *csgG* gene encodes a protein that governs the stability and secretion of the structural proteins CsgA and CsgB.[13] The *csgD* gene encodes a transcriptional activator that manages the expression of the curli operons.[29] Loss of CsgD results in a lower number of curli and altered initial bacterial adhesion dynamics.[13,24] Curli plays a role only during the initial adhesion process, and then are silenced as the Cpx and Rcs pathways switch on in subsequent biofilm formation stages. Furthermore, we examined the changes that are associated with deletions of two major flagellar genes, *fliC*, which encodes flagellin the major structural component of flagella,[30,9] and *flgE*, which encodes the hook connection for the flagella protein to the cell body.[30,31] Finally, we assessed deletion mutants of two genes that encode enzymes necessary for the proper secretion of the LPS: *gmhB* and *rfaH*.[32−34] Prior work has reported that deletion of both of these genes can lead to changes in *E. coli* adhesion.[32]

Figure 1 summarizes all the measured zeta potential values for the different *E. coli* strains. Three mutations (Δ*fimH*, Δ*csgG*, and Δ*fliC*) exhibited significant changes to their zeta

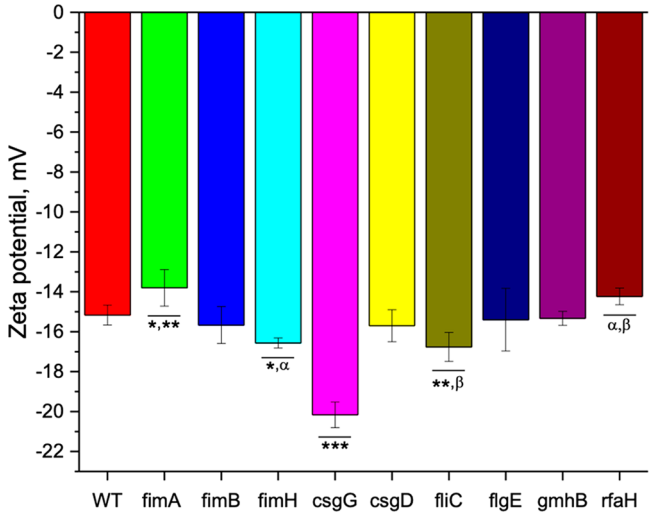

Figure 1. Summary of the average zeta potential values. Measurements were taken for 10 strains. Statistical analysis shows significant differences among certain samples marked on the graph. The notation * indicates a significant statistical difference between *fimA* and *fimH* strains, **, between *fimA* and *fliC*; *α*, between *fimH* and *rfaH*; *β*, between *fimH* and *rfaH*; *** indicates that the *csgG* strain zeta potential was significantly different compared to all other tested strains.

DOI: 10.1021/acsabm.9b00573
ACS Appl. Bio Mater. 2019, 2, 4044−4051

potential in comparison to the values obtained for the wild-type (WT) bacteria. Larger zeta potential values are indicative of more stable dispersion of bacteria in solution. The recorded significant differences in zeta potential values supports the notion that the deletions in the above three mutant strains are changing the surface physio-chemical properties and can lead to more cell−cell aggregation. Changes in zeta potential are also associated with alterations in the cell surface permeability that can lead to differences in functions essential for cell survival.[35] It is important to note that mutations associated with altering the cell wall via LPS resulted in the smallest change in zeta potential. Also, we need to state that there is no consistent correlation between the zeta potential changes observed in the *E. coli* mutants and the alteration of bacterial behavior on UV+ GaN semiconductor materials. Although ΔcgsG bacteria had a significant reduction in zeta potential and the largest increase in adhesion to UV+ GaN surfaces; Δflic, which also demonstrated a significant reduction in zeta potential, exhibited reduced adhesion to UV+ GaN materials. These results suggest that a reduced zeta potential surface does not control the changes to the bacteria adhesion but may contribute to the essential roles that morphological structures like flagella have in processes like adhesion. ΔcgsG mutants have a wild-type flic gene and normal flagella. It is possible that the alteration of the cell wall in the ΔcgsG mutant bacteria changes the surface charge, which then enhances flagellar-based adhesion,[8,9] and bacterial cells that are missing flagella simply do not adhere to GaN surfaces regardless of the changes to their surface charge. In future experiments, double mutant bacteria, ΔcgsG and Δflic, will allow us to test such hypotheses.

There is also a possibility that certain types of chemical moieties tested in this study become more accessible due to the loss of specific surface structures due to the mutation. Bacteria are inherently negatively charged since their outermost layer is made of peptidoglycan, a mixture of carboxyl and amine groups.[6,33] We performed additional measurements to compare the hydrophobicity of these strains using a standard microbial adhesion to hydrocarbon (MATH) assay.[36] In this assay, one compares initial and final bacterial concentrations after samples are placed in contact with a hydrocarbon solution. This assay avoids issues associated with drying bacteria on surfaces with variable defects that might cause inconsistences in the measurements. The MATH assay results are summarized in Table 2. Significant changes in the % hydrophobicity were observed in the following cases: Δ*fimA*, Δ*csgD*, Δ*csgG*, and Δ*rfaH*. The results show that mutations in the surface structures associated with adhesive fimbriae and curli significantly increase the % hydrophobicity (in some instances, to 2 to 5 times greater values). In contrast, mutations in the LPS cause relatively small deviations in the % hydrophobicity compared to WT.

2.2. Semiconductor Interfaces. We have reported on a number of detailed GaN characterization studies.[17] In particular, we have examined changes in the surface chemistry and roughness via spectroscopy and microscopy analysis.[37] In this study, we quantified the surface potential changes of the batch of Ga-polar GaN utilized for the biofilm behavior studies. All surface potential data were collected with KPFM[38] as described in the Experimental Section. Figure 2a shows the KPFM data as a function of time prior to UV light exposure, during UV light illumination, and after the light source was turned off. Figure 2b contrasts the average surface potential values (in mV) under the two experimental conditions. The KPFM data indicates that the surface potential sharply increases upon illumination and decays slowly when the light is removed. The initial potential values are in the range of 200−300 mV. Irradiating the samples with the UV light increases the surface potential up to 1−1.1 V, which corresponds to approximately 850 mV increase or 3.4 times larger values than the initial values. The data indicates that it takes 360 s (or 6 min) for the surface potential to decrease and then equilibrate after the light source is removed. After the UV irradiation, the surface potential drops to ∼160−210 mV, which corresponds to a drop of 60 mV or approximately 25% decrease from the values recorded at the beginning of the experiments. The detected difference may be considered to be biologically significant. This change is in the range of many biologically relevant membrane-based signaling systems such as these found in neurons. Such systems have been shown to respond to changes in a few millivolts. The ways of interpreting surface potential data are widely discussed in the literature.[39] It is significant to note that the surface potential takes time to decay upon removal of light, since during the *E. coli* experiments, we never exposed the cells directly to the light and used the GaN samples after UV illumination. Considering the charge decay speed, one should notice that the response of the bacteria to change surface charge may persist and/or be delayed due to the time scales of physiological and/or genetic responses, i.e., the reset of the bacteria may not be rapid. However, it cannot be ruled out that other changes such as the increase in Ga+ or ROS may also contribute to bacterial reactions observed.

Table 2. Summary of the % Hydrophobicity Measurements Performed with All the *E. coli* Strains Used in This Work

gene	bacterial component/function	% hydrophobicity[a]
wild-type		5 ± 0.04
Δ*fimA*	Fimbriae/major repeating subunit	10.53 ± 0.09#
Δ*fimB*	Fimbriae/transcriptional regulator of fimA	2.83 ± 5.72
Δ*fimH*	Fimbriae/a minor protein component that recognizes mannosyl residues	5.72 ± 0.05
Δ*csgD*	Curli/DNA-binding transcriptional activator in 2-component regulatory system	26.3 ± 0.14#
Δ*csgG*	Curli/outer-membrane lipoprotein required for curli subunit secretion	9.45 ± 0.05#
Δ*FliC*	Flagella/main structural subunit	10.99 ± 0.12#
Δ*FlgE*	Flagella/connects filament to main bacterial body	3.84 ± 0.03#
Δ*gmhB*	LPS/enzyme required for LPS-synthesis	6 ± 0.09
Δ*rfaH*	LPS/core synthesis and O-antigen attachment	2.82 ± 0.02#

[a]#$P < 0.05$.

An additional characterization performed on the semiconductor interfaces involved assessment of their hydrophobicity. Literature studies have pointed to the importance of surface hydrophobicity with respect to adhesion of certain cell types.[40] In our prior work, XPS analysis concluded that the surface composition of the GaN is not statistically different before or after exposure to UV light.[37] Figure 3 summarizes all the contact angle measurements recorded during the different experimental conditions as detailed in the Experimental Section. The clean GaN surface equilibrated in air is moderately hydrophobic with a contact angle below 60°, and there are no significant changes before and after UV illumination in air, as well as after incubation in buffer or

DOI: 10.1021/acsabm.9b00573
ACS Appl. Bio Mater. 2019, 2, 4044−4051

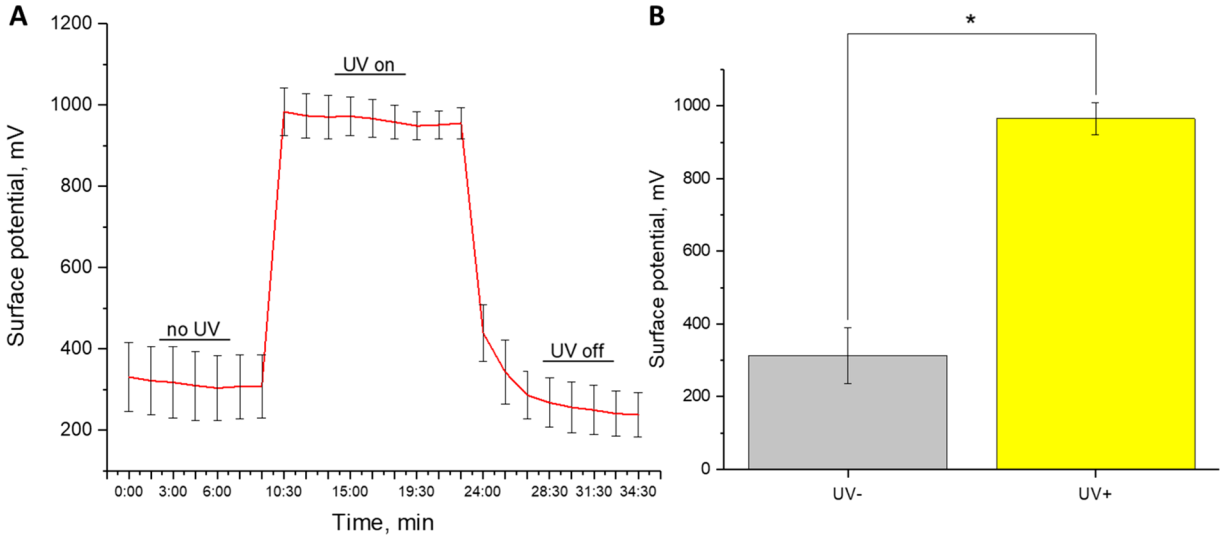

Figure 2. (a) Surface potential (mV) vs time (min) under various external conditions (equilibrated sample not exposed to UV light, UV on, and UV off). (b) Summary of average surface potential values (mV) before (UV-) and after (UV+) exposure to UV light.

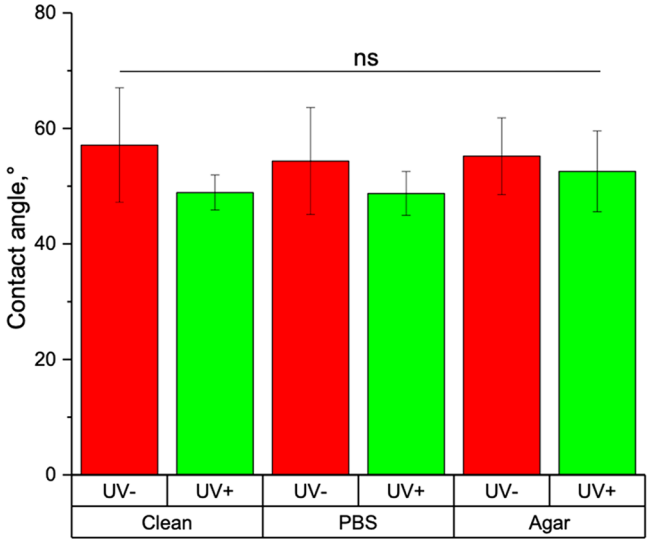

Figure 3. Average contact angle values for GaN samples before (UV-) and after (UV+) light irradiation and different treatments: clean, after PBS incubation for 1 h, and after placement in agar for 1 h. All samples were dried prior to the contact angle measurements which were performed with droplets of DI water as described in the Experimental Section.

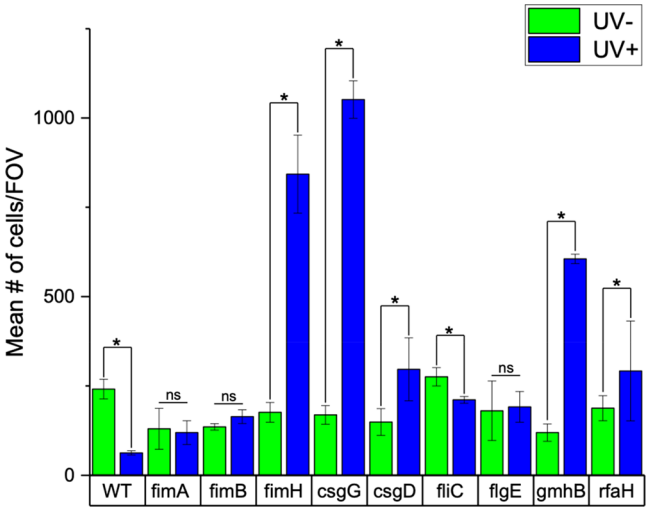

Figure 4. Summary of averaged adhesion assay tests. Biofilms of 10 strains of *E. coli* were grown on nonirradiated (UV-) and UV-irradiated (UV+) GaN samples. Carried statistical analysis shows significant differences in cases indicated by the *.

agar broth. Thus, any changes we observe in the different *E. coli* strain behavior on GaN before and after UV light treatment of the material cannot be rationalized due to differences in the inorganic interface hydrophobicity.

2.3. *E. coli* Behavior on Semiconductor Interfaces. We initially compared the adhesion behavior of all 10 *E. coli* strains to GaN surfaces that were either UV irradiated or not. These results are summarized in Figure 4. We observed a reduction of cell−substrate adhesion with the wild-type *E. coli* cells on GaN surfaces that have been treated with UV light. This result is similar to the interaction of other microbes such as the budding yeast *Saccharomyces cerevisiae* and the Gram-negative bacteria *Pseudomonas aeruginosa* when their behavior on UV treated and nontreated GaN is compared.[20,37] Our current analysis tools prevent us from determining if this observation is due to the physical alteration of the local environment such as a reduction in positive charge on the surface or due to an active response from the bacteria itself. In some mutant bacteria (Δ*fimA*, Δ*fimB*, and Δ*flgE*), we see a reduction in surface binding when compared to WT and a lack of any difference in the response to the variably treated GaN. Comparing the adhesion trends of the bacterial strains on uncharged and charged surfaces shows that only the WT and Δ*fliC* strains show a significant decrease in the total retention of bacteria between these two conditions. Several other mutants (Δ*fimH*, Δ*csgG*, Δ*csgD*, Δ*gmhB*, Δ*rfaH*) show the opposite response, increased binding to charged GaN surfaces when compared to WT. There was a 4-fold increase of retention of Δ*fimH E. coli*, 5-fold increase of Δ*csgG*, and a 3-fold increase of Δ*gmhB* (Figure 4). The adhesion results do not show a direct correlation with either bacterial zeta potential or % hydrophobicity. This observation supports the notion that the loss of specific bacterial surface structures lead to interfacial

DOI: 10.1021/acsabm.9b00573
ACS Appl. Bio Mater. 2019, 2, 4044−4051

interactions that are primarily facilitated by the semiconductor interface charge but are too complex to be rationalized by methods such as zeta potential and MATH assay that rely on indirect measurements to calculate the desired parameters.[41] Thus, increased surface charge is one of several characterized physicochemical changes at the GaN interface that can be controlling bacterial behavior. Bacteria have been shown to respond to a variety of signals and extracellular cues including surface morphology and structure.[2−4] Often, these responses are mediated by specific morphological features including flagella and fimbriae. While we do not find a global relationship between the alteration of cell hydrophobicity or zeta potential and cell behavior on GaN material, these results demonstrate that specific alteration to the cell via mutation can alter the cell physical properties, and that in the right context, i.e., cells bearing wild-type morphological features, these changes may alter the behavior on GaN materials.

During the collection of data associated with adhesion, we observed that the WT bacteria displayed a different motility on the UV-treated vs untreated surface. The WT bacteria were immobile on the UV+ GaN, whereas they showed regular movement on UV- GaN. The mutants also showed this type of behavior difference on the two types of semiconductor interfaces. While some of the genes that were used in this study are responsible for twitching and swimming motion,[42] the uniform loss of motility suggests that the reduction of motive force leads to slower pili action and, therefore, slow bacteria.[43] The data on Figure 4 and the motility trends support the notion that the adhesion to the surface is not facilitated by the ability to move. Rather, an increased adhesion (the case for Δ*fimH*, Δ*csgG*, Δ*csgD*, Δ*gmhB*, Δ*rfaH*) results from an initially favorable interaction between the charged semiconductor interface and the *E. coli* cell surface with specific morphology.

Loss of the *E. coli* surface structure due to mutations like those studied here result in changes to its membrane potential (ΔΨ).[44] Here, we quantify ΔΨ for all mutants on UV-treated and nontreated GaN (Figure 5). We used the ratiometric dye

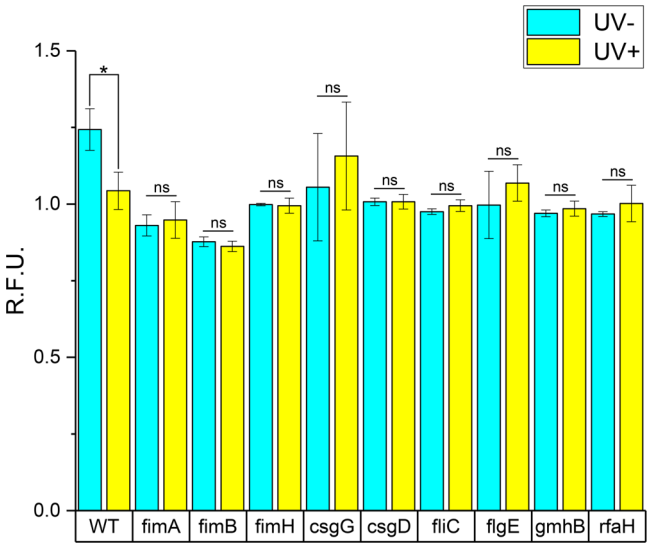

Figure 5. Comparison of *E. coli* membrane potential assay test results. Biofilms were grown on nonirradiated (UV-) and UV-irradiated (UV +) GaN samples. Statistical analysis unveils a significant difference in the wild-type case on UV+ and UV- surfaces.

DiOC(3) on bacteria exposed to UV+ and UV- GaN surfaces. The DiOC(3) dye is sequestered in cells with normal proton motive force; if the membrane potential is altered, there will be a shift from green to red fluorescence. The ratio of the green to red fluorescence was calculated for WT. Higher ratiometric values correspond to lower membrane potential (Ψ). A radical change in membrane potential was seen for wild-type *E. coli* placed on UV+ and UV- GaN (Figure 5). We noticed that the membrane potentials of all the mutant strains grown on the uncharged surfaces were lower than that of the WT. Using the results obtained as baseline membrane potentials for the individual strains, we compared their membrane potential to that when grown on the UV+ surfaces. In stark contrast to the ΔΨ of the WT, all the mutant strains showed little to no change in membrane potentials upon comparison between UV + and UV-. Research with nanostructured materials has shown that mechanosensitive events will disrupt the membrane potential of bacteria and other microbes.[45] Contact with any type of interface is a mechanosensitive event. Changes induced by the mutations in genes associated with bacterial cell surface composition and/or structure are expected to play a critical role in any function associated with mechanical properties recognition such as adhesion.[38,46] The fact that no differences were recorded in the Ψ data for the mutants compared to the wild-type for UV- and UV+ GaN leads us to conclude that mutations to the appendages decreases the mechanical sensitivity of *E. coli* toward recognition of the variable inorganic interfaces. The interesting aspect is that this loss of membrane potential change is uniform in *E. coli* strains that have diverse alterations to their surface morphologies; this suggests that either these diverse processes share a common response mechanism or the response to the UV+ is extremely sensitive, and any change to surface/cell interactions results in a refractory membrane potential response.

The *E. coli* cell wall has a number of components that participate in so-called defense mechanisms against unfavorable conditions.[47] Catalase enzyme is responsible for the elimination of harmful reactive oxygen species (ROS).[48] We evaluated the amount of catalase activity for all mutants on different interfaces (Figure 6). In instances where there is a statistically significant difference in the catalase activity between UV-treated and nontreated samples, there is a decrease in the enzyme activity. We have documented that UV exposure of GaN can lead to more oxides on the surface,[37] but despite this, the catalase data indicates that there is a decrease of the amount of catalysis associated with conversion of ROS inside the cells. Mutants associated with fimbriae alterations showed no difference in catalase activity between UV+ and UV-. Our data is in agreement with prior work that found that initial biofilm formation is more sensitive to pathways govern by CsgDu.[23]

3. CONCLUSIONS

In summary, we characterized the behavior of 10 different *E. coli* strains on GaN interfaces with variable surface potential. In wild-type *E. coli*, we observed changes in bacterial behavior in response to changes in surface charge of the GaN substrate. This behavior was altered due to mutations in genes that encoded specific components of the *E. coli* cell exterior. We found radical alteration to wild-type behavior in mutant *E. coli*, particularly those that influence the composition and structure of the cell wall. While wild-type *E. coli* exhibited reduced affinity to the charged GaN interface, we observed an increase

DOI: 10.1021/acsabm.9b00573
ACS Appl. Bio Mater. 2019, 2, 4044−4051

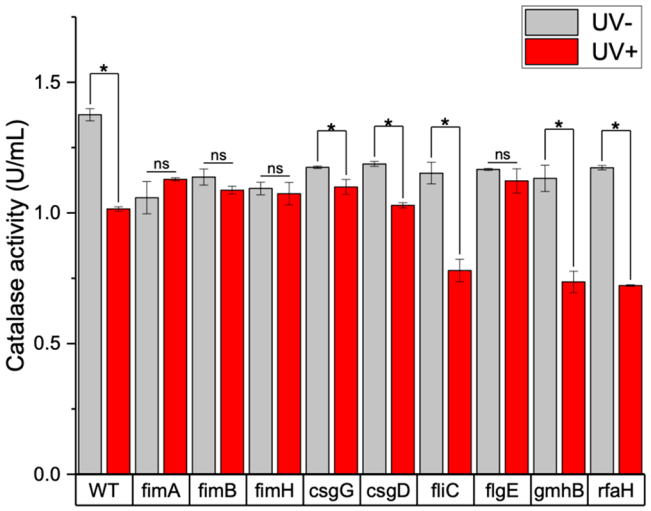

Figure 6. Comparison of the catalase activity of *E. coli* biofilms formed on GaN surfaces. Certain strains (indicated with *) exhibited a statistical difference in the amount of catalase when biolayers were grown on nonirradiated (UV-) vs UV-irradiated (UV+) substrates.

in bacterial adhesion to the UV-irradiated GaN samples using the following strains: Δ*csgG*, Δ*csgD*, Δ*gmhB*, and Δ*rfaH*, all of which encode components of the peptidoglycan. Furthermore, we also observe increased affinity in Δ*fimH E. coli* a critical component for alternative modes of motility and surface colonization. Furthermore, the quantitative assays for catalase and membrane potential showed that the wild type is more sensitive to the variable semiconductor interfaces compared to the mutants. The results of this work will be of practical interest to researchers in the bioelectronics field.

4. EXPERIMENTAL SECTION

Semiconductor Surfaces. Ga-polar GaN was grown as reported in previous publicationss.[49−51] The surfaces utilized here were from the same batch used for earlier work and additional materials characterization has already been reported.[37] As in previous studies, the UV-irradiation of clean equilibrated GaN samples in all experiments was performed for 1 h.

AFM Characterization. All of the AFM and KPFM work was performed on Oxford Instruments MFP-3D Origin. Experimental details and statistical analysis descriptions have been published by our groups.[19,21]

Contact Angle Measurements. All data were collected with a Ramé-Hart automated dispensing system and a Ramé-Hart Model 200 F4 series goniometer. The droplets deposited had a 1.25 μL volume. The droplets were imaged and analyzed with OnScreenProtractor Java-applet (v 0.5).

Bacterial Strains and Growth Conditions. All *E. coli* strains were obtained from the Keio library[52] with a single deletion mutation from the parent BW25113 strain. Before each characterization and biofilm formation described in this work, a fresh bacterial colony was seeded from a mother plate and cultured overnight in Luria Broth medium. All growth was carried out in a shaker incubator at 37 °C.

Bacterial Surface Characterization. Prior to data collection, the bacterial cultures were grown overnight and then diluted to an OD_{600} ∼0.1. Subsequently, 750 μL of the culture was added to a cuvette followed by the dip cell electrode. All zeta potential measurements were collected with a Malvern Zetasizer Nano ZS. The relative hydrophilicity was derived using a standard MATH assay.[36] Briefly, each measurement was done with the following procedure: 5 mL of overnight cultures of the bacterial cells were pelleted, resuspended in 1×PBS, and diluted to an OD_{600} of ∼0.1. The OD_{600} value of the preprocessed sample was recorded. Next, 1 mL of octane was added to 4 mL of each of the bacterial cultures. These were then vortexed vigorously for 2 min and allowed to stand for 20 min. The OD_{600} value of the aqueous part of the cultures was recorded each time. The following formula was utilized in all calculations to determine the relative hydrophobicity of each bacterial knockout strain:

$$\%\text{hydrophobicity} = \left(1 - \frac{OD_{600}\text{before}}{OD_{600}\text{after}}\right) \times 100$$

Adhesion Assay. A bacterial adhesion assay was performed on a Zeiss inverted spinning disc confocal microscope via the direct microscopic count (DMC) method. For each experiment, cells were grown overnight at 37 °C in a shaker incubator and adjusted to an OD_{600} of ∼0.1. The following day, 100 μL of the OD_{600} adjusted bacterial cells were incubated with SYTO9 in the dark at room temperature (∼23 °C) for 20 min. The cell−dye combination was pelleted and resuspended in 1 mL 1×PBS. Next, 100 μL of labeled bacteria was incubated in both UV treated and nontreated GaN substrates for 5 min at room temperature. All substrates were then gently washed with 1×PBS and immediately imaged. The number of bacteria per field of view (FOV) at 100× magnification was recorded on each semiconductor sample. The data reported is extracted from at least 15 images per sample. All experimental conditions were repeated three times.

Membrane Potential Assay. A Baclight Bacterial Membrane Potential Kit (Thermo Scientific; catalog number B34590) was utilized according to the manufacturer's protocol. A working solution of the stock membrane potential monitoring dye [3 mM $DiOC_2(3)$] was prepared by diluting 1 μL of the stock solution in 1 mL of sterilized PBS. 10 μL of this working solution was then added to the cells. A solution of carbonyl cyanide 3-chlorophenylhydrazone (CCCP) was similarly diluted. Cells were grown overnight at 37 °C in a shaker incubator. The next day, they were adjusted to an OD_{600} of 0.05 and allowed to grow to OD_{600} = 0.6. Subsequently, 100 μL of this cell culture was pelleted and resuspended in 1 mL PBS. A control tube containing cells but no dye was kept aside. 10 μL of the $DiOC_2(3)$ working solution was then added to 1 mL of cells in PBS. 100 μL of this cell−dye solution was added to each substrate in a 96-well plate and allowed to incubate at room temperature for 30 min. The CCCP working solution was added to the cell culture tube and utilized as a positive control. PBS with the dye solution/no cells and PBS solution/no cells were used as negative controls along with a well containing cells but no dye. The working CCCP solution was added to the working dye solution as a control for dissipating membrane potential. Semiconductor surfaces, both treated and nontreated with UV light, were added to the solutions described above. After the 30 min incubation period, the GaN substrates were carefully removed using forceps and placed upside-down on a coverslip and imaged using a Zeiss inverted spinning disc confocal microscope. At least 15 images were taken per sample. The experiment was repeated three times with at least two different overnight bacterial cultures.

Catalase Activity Assay. The catalase colorimetric activity kit from Thermo Fisher (catalog number: EIACATC) was utilized according to the supplied protocol. A catalase standard was provided to generate a standard curve. The *E. coli* cultures were grown overnight and diluted to an OD_{600} of 0.1. Subsequently, 100 μL aliquots were added to the UV treated and nontreated GaN surfaces. The cells were then vortexed loose from the surface of the GaN and diluted in the assay buffer, 25 μL of which was added to the wells of a 96-well plate. 25 μL of hydrogen peroxide (H_2O_2) was then added to each well and left to incubate at room temperature for 30 min. 25 μL of the provided substrate and horseradish peroxidase (HRP) were then added and left to incubate further for 15 min. The HRP and substrate reacted to form a pink solution. The 96-well plate was then read spectrophotometrically at OD_{560}. An increase in catalase activity is seen by the decrease in pinkness of the samples, which indicates a decrease in the amount of H_2O_2. The number of units of catalase present in each sample was calculated using the initially generated standard curve. Each unit of catalase corresponds to the decomposition of 1 μmol of H_2O_2 per minute at room temperature.

DOI: 10.1021/acsabm.9b00573
ACS Appl. Bio Mater. 2019, 2, 4044−4051

Statistical Analysis. All experiments, including materials characterization, have been repeated at least 3 times. The reported analysis was performed utilizing 1-way, 2-way, and 3-way ANOVA methods and a commercial software package OriginPro 2017 (v 9.4.1.354).

■ ASSOCIATED CONTENT

Supporting Information

The Supporting Information is available free of charge on the ACS Publications website at DOI: 10.1021/acsabm.9b00573.

Additional characterization and data analysis (PDF)

■ AUTHOR INFORMATION

Corresponding Authors

*E-mail: drlajeun@uncg.edu.
*E-mail: ivanisevic@ncsu.edu.

ORCID

Pramod Reddy: 0000-0002-8556-1178
Dennis R. LaJeunesse: 0000-0001-5049-8968
Albena Ivanisevic: 0000-0003-0336-1170

Notes

The authors declare no competing financial interest.

■ ACKNOWLEDGMENTS

We thank Army Research Office under W911NF1910033 for support of this work. Partial financial support from NSF (ECCS-1653383) is greatly appreciated.

■ REFERENCES

(1) Kung, C. A possible unifying principle for mechanosensation. *Nature* **2005**, *436* (7051), 647−654.
(2) Startek, J. B.; Boonen, B.; Talavera, K.; Meseguer, V. TRP Channels as Sensors of Chemically-Induced Changes in Cell Membrane Mechanical Properties. *Int. J. Mol. Sci.* **2019**, *20* (2), 371.
(3) Van Houdt, R.; Michiels, C. W. Role of bacterial cell surface structures in Escherichia coli biofilm formation. *Res. Microbiol.* **2005**, *156* (5), 626−633.
(4) Tuson, H. H.; Weibel, D. B. Bacteria-surface interactions. *Soft Matter* **2013**, *9* (18), 4368−4380.
(5) Tallawi, M.; Opitz, M.; Lieleg, O. Modulation of the mechanical properties of bacterial biofilms in response to environmental challenges. *Biomater. Sci.* **2017**, *5* (5), 887−900.
(6) Klein, G; Raina, S. Regulated Assembly of LPS, Its Structural Alterations and Cellular Response to LPS Defects. *Int. J. Mol. Sci.* **2019**, *20* (2), 356.
(7) Dahlquist, F. W. The Bacterial Flagellar Motor Continues to Amaze. *Biophys. J.* **2018**, *114* (3), 505−506.
(8) Berg, H. C. The flagellar motor adapts, optimizing bacterial behavior. *Protein Sci.* **2017**, *26* (7), 1249−1251.
(9) Evans, L. D. B.; Hughes, C.; Fraser, G. M. Building a flagellum outside the bacterial cell. *Trends Microbiol.* **2014**, *22* (10), 566−572.
(10) Schwan, W. R.; Shibata, S.; Aizawa, S.-I.; Wolfe, A. J. The two-component response regulator RcsB regulates type 1 piliation in Escherichia coli. *J. Bacteriol.* **2007**, *189* (19), 7159−7163.
(11) Allen, W. J.; Phan, G.; Waksman, G. Pilus biogenesis at the outer membrane of Gram-negative bacterial pathogens. *Curr. Opin. Struct. Biol.* **2012**, *22* (4), 500−506.
(12) Evans, M. L.; Chapman, M. R. Curli biogenesis: order out of disorder. *Biochim. Biophys. Acta, Mol. Cell Res.* **2014**, *1843* (8), 1551−1558.
(13) Barnhart, M. M.; Chapman, M. R. Curli Biogenesis and Function. *Annu. Rev. Microbiol.* **2006**, *60* (1), 131−147.
(14) Rizzello, L.; Cingolani, R.; Pompa, P. P. Nanotechnology tools for antibacterial materials. *Nanomedicine* **2013**, *8* (5), 807−821.
(15) Macedo, L. J. A.; Iost, R. M.; Hassan, A.; Balasubramanian, K.; Crespilho, F. N. Bioelectronics and Interfaces Using Monolayer Graphene. *ChemElectroChem* **2019**, *6* (1), 31−59.
(16) Lovley, D. R. Electromicrobiology. *Annu. Rev. Microbiol.* **2012**, *66* (1), 391−409.
(17) Snyder, P. J.; Reddy, P.; Kirste, R.; Collazo, R.; Ivanisevic, A. Bulk and Surface Electronic Properties of Inorganic Materials: Tools to Guide Cellular Behavior. *Small Methods.* **2018**, *2* (9), 1800016.
(18) Snyder, P. J.; Kirste, R.; Collazo, R.; Ivanisevic, A. Nanoscale topography, semiconductor polarity and surface functionalization: additive and cooperative effects on PC12 cell behavior. *RSC Adv.* **2016**, *6* (100), 97873−97881.
(19) Snyder, P. J.; Reddy, P.; Kirste, R.; Lajeunesse, D. R.; Collazo, R.; Ivanisevic, A. Noninvasive Stimulation of Neurotypic Cells Using Persistent Photoconductivity of Gallium Nitride. *ACS Omega.* **2018**, *3* (1), 615−621.
(20) Snyder, P. J.; Lajeunesse, D. R.; Reddy, P.; Kirste, R.; Collazo, R.; Ivanisevic, A. Bioelectronics communication: encoding yeast regulatory responses using nanostructured gallium nitride thin films. *Nanoscale* **2018**, *10* (24), 11506−11516.
(21) Snyder, P. J.; Reddy, P.; Kirste, R.; LaJeunesse, D. R.; Collazo, R.; Ivanisevic, A. Variably doped nanostructured gallium nitride surfaces can serve as biointerfaces for neurotypic PC12 cells and alter their behavior. *RSC Adv.* **2018**, *8* (64), 36722−36730.
(22) Gualdi, L.; Tagliabue, L.; Bertagnoli, S.; Ieranò, T.; De Castro, C.; Landini, P. Cellulose modulates biofilm formation by counteracting curli-mediated colonization of solid surfaces in Escherichia coli. *Microbiology* **2008**, *154* (7), 2017−2024.
(23) Prigent-Combaret, C.; Brombacher, E.; Vidal, O.; Ambert, A.; Lejeune, P.; Landini, P.; Dorel, C. Complex regulatory network controls initial adhesion and biofilm formation in Escherichia coli via regulation of the csgD gene. *J. Bacteriol.* **2001**, *183* (24), 7213−7223.
(24) Pesavento, C.; Becker, G.; Sommerfeldt, N.; Possling, A.; Tschowri, N.; Mehlis, A.; Henggre, R. Inverse regulatory coordination of motility and curli-mediated adhesion in Escherichia coli. *Genes Dev.* **2008**, *22* (17), 2434−2446.
(25) Hughes, K. T.; Berg, H. C. The bacterium has landed. *Science* **2017**, *358* (6362), 446−447.
(26) Friedlander, R. S.; Vlamakis, H.; Kim, P.; Khan, M.; Kolter, R.; Aizenberg, J. Bacterial flagella explore microscale hummocks and hollows to increase adhesion. *Proc. Natl. Acad. Sci. U. S. A.* **2013**, *110* (14), 5624−5629.
(27) Schwan, W. R. Regulation of fim genes in uropathogenic Escherichia coli. *World J. Clin Infect Dis.* **2011**, *1* (1), 17−25.
(28) Anderson, B. N.; Ding, A. M.; Nilsson, L. M.; Kusuma, K.; Tchesnokova, V.; Vogel, V.; Sokurenko, E. V.; Thomas, W. E. Weak rolling adhesion enhances bacterial surface colonization. *J. Bacteriol.* **2007**, *189* (5), 1794−1802.
(29) Ogasawara, H.; Yamada, K.; Kori, A.; Yamamoto, K.; Ishihama, A. Regulation of the Escherichia coli csgD promoter: interplay between five transcription factors. *Microbiology* **2010**, *156* (8), 2470−2483.
(30) Haiko, J.; Westerlund-Wikström, B. The role of the bacterial flagellum in adhesion and virulence. *Biology (Basel, Switz.)* **2013**, *2* (4), 1242−1267.
(31) Minamino, T.; Imada, K. The bacterial flagellar motor and its structural diversity. *Trends Microbiol.* **2015**, *23* (5), 267−274.
(32) Niba, E. T. E.; Naka, Y.; Nagase, M.; Mori, H.; Kitakawa, M. A genome-wide approach to identify the genes involved in biofilm formation in E. coli. *DNA Res.* **2008**, *14* (6), 237−246.
(33) Taylor, P. L.; Sugiman-Marangos, S.; Zhang, K.; Valvano, M. A.; Wright, G. D.; Junop, M. S. Structural and Kinetic Characterization of the LPS Biosynthetic Enzyme d-α,β-d-Heptose-1,7-bisphosphate Phosphatase (GmhB) from Escherichia coli. *Biochemistry* **2010**, *49* (5), 1033−1041.
(34) Beloin, C.; Michaelis, K.; Lindner, K.; Landini, P.; Hacker, J.; Ghigo, J.; Dobrindt, U. The transcriptional antiterminator RfaH represses biofilm formation in Escherichia coli. *J. Bacteriol.* **2006**, *188* (4), 1316−1331.

DOI: 10.1021/acsabm.9b00573
ACS Appl. Bio Mater. 2019, 2, 4044−4051

(35) Halder, S.; Yadav, K. K.; Sarkar, R.; Mukherjee, S.; Saha, P.; Haldar, S.; Karmakar, S.; Sen, T. Alteration of Zeta potential and membrane permeability in bacteria: a study with cationic agents. *SpringerPlus* **2015**, *4*, 672.
(36) Zoueki, C. W.; Tufenkji, N.; Ghoshal, S. A modified microbial adhesion to hydrocarbons assay to account for the presence of hydrocarbon droplets. *J. Colloid Interface Sci.* **2010**, *344* (2), 492−496.
(37) Gulyuk, V. A.; LaJeunesse, D. R.; Collazo, R.; Ivanisevic, A. Characterization of Pseudomonas aeruginosa Films on Different Inorganic Surfaces before and after UV Light Exposure. *Langmuir* **2018**, *34* (36), 10806−10815.
(38) Birkenhauer, E.; Neethirajan, S. Surface potential measurement of bacteria using Kelvin probe force microscopy. *J. Visualized Exp.* **2014**, No. 93, e52327−e52327.
(39) Belianinov, A.; Vasudevan, R.; Strelcov, E.; et al. Big data and deep data in scanning and electron microscopies: deriving functionality from multidimensional data sets. *Adv. Struct Chem. Imaging.* **2015**, DOI: 10.1186/s40679-015-0006-6.
(40) Donlan, R. M. Biofilms: microbial life on surfaces. *Emerging Infect. Dis.* **2002**, *8* (9), 881−890.
(41) Skoglund, S.; Hedberg, J.; Yunda, E.; Godymchuk, A.; Blomberg, E.; Odnevall Wallinder, I. Difficulties and flaws in performing accurate determinations of zeta potentials of metal nanoparticles in complex solutions-Four case studies. *PLoS One* **2017**, *12* (7), e0181735−e0181735.
(42) Zhang, R.; Ni, L.; Jin, Z.; Li, J.; Jin, F. Bacteria slingshot more on soft surfaces. *Nat. Commun.* **2014**, *5*, 5541.
(43) Hospenthal, M. K.; Costa, T. R. D.; Waksman, G. A comprehensive guide to pilus biogenesis in Gram-negative bacteria. *Nat. Rev. Microbiol.* **2017**, *15*, 365.
(44) Zilberstein, D.; Agmon, V.; Schuldiner, S.; Padan, E. Escherichia coli intracellular pH, membrane potential, and cell growth. *J. Bacteriol.* **1984**, *158* (1), 246−252.
(45) Kaweeteerawat, C.; Chang, C. H.; Roy, K. R.; Lui, R.; Li, R.; Toso, D.; Fischer, H.; Ivask, A.; Ji, Z.; Zink, J. I.; Zhou, Z. H.; Chanfreau, G. F.; Telesca, D.; Cohen, Y.; Holden, P. A.; Nel, A. E.; Godwin, H. A. Cu Nanoparticles Have Different Impacts in Escherichia coli and Lactobacillus brevis than Their Microsized and Ionic Analogues. *ACS Nano* **2015**, *9* (7), 7215−7225.
(46) Harapanahalli, A. K.; Younes, J. A.; Allan, E.; van der Mei, H. C.; Busscher, H. J. Chemical Signals and Mechanosensing in Bacterial Responses to Their Environment. *PLoS Pathog.* **2015**, *11* (8), No. e1005057.
(47) Ravindra Kumar, S.; Imlay, J. A. How Escherichia coli tolerates profuse hydrogen peroxide formation by a catabolic pathway. *J. Bacteriol.* **2013**, *195* (20), 4569−4579.
(48) Schellhorn, H. E. Regulation of hydroperoxidase (catalase) expression in Escherichia coli. *FEMS Microbiol. Lett.* **1995**, *131* (2), 113−119.
(49) Kirste, R.; Mita, S.; Hussey, L.; Hoffmann, M.; Guo, W.; Bryan, I.; Bryan, Z.; Tweedie, J.; Xie, J.; Gerhold, M.; Collazo, R.; Sitar, Z. Polarity control and growth of lateral polarity structures in AlN. *Appl. Phys. Lett.* **2013**, *102* (18), 181913.
(50) Liu, F.; Collazo, R.; Mita, S.; Sitar, Z.; Duscher, G.; Pennycook, S. J. The mechanism for polarity inversion of GaN via a thin AlN layer: Direct experimental evidence. *Appl. Phys. Lett.* **2007**, *91* (20), 203115.
(51) Collazo, R.; Mita, S.; Aleksov, A.; Schlesser, R.; Sitar, Z. Growth of Ga- and N- polar gallium nitride layers by metalorganic vapor phase epitaxy on sapphire wafers. *J. Cryst. Growth* **2006**, *287*, 586−590.
(52) Baba, T.; Ara, T.; Hasegawa, M.; Okumura, Y.; Baba, M.; Datsenko, K.; Tomita, M.; Wanner, B.; Mori, H. Construction of Escherichia coli; K-12 in-frame, single-gene knockout mutants: the Keio collection. *Mol. Syst. Biol.* **2006**, *2* (1), 1 DOI: 10.1038/msb4100050.

DOI: 10.1021/acsabm.9b00573
ACS Appl. Bio Mater. 2019, 2, 4044−4051